Grazing Exit Electron Probe Microanalysis of Submicrometer Inclusions in Metallic Materials

ARTICLE *in* ANALYTICAL CHEMISTRY · SEPTEMBER 2003

Impact Factor: 5.64 · DOI: 10.1021/ac020740l · Source: PubMed

6 AUTHORS, INCLUDING:

Tohru Awane
Kyushu University
26 PUBLICATIONS **71** CITATIONS
SEE PROFILE

Nobuhiro Ishikawa
National Institute for Materials Science
24 PUBLICATIONS **213** CITATIONS
SEE PROFILE

Shigeo Tanuma
National Institute for Materials Science
133 PUBLICATIONS **4,210** CITATIONS
SEE PROFILE

Anal. Chem. **2003,** *75,* 3831−3836

Grazing Exit Electron Probe Microanalysis of Submicrometer Inclusions in Metallic Materials

Tohru Awane,* Takashi Kimura, Kenji Nishida, Nobuhiro Ishikawa, Shigeo Tanuma, and Morihiko Nakamura

Materials Analysis Station, National Institute for Materials Science, 1-2-1 Sengen, Tsukuba, Ibaraki 305-0047, Japan

Grazing exit electron probe microanalysis (GE-EPMA) is a new method of EPMA in which characteristic X-rays emitted from only near-surface regions of a specimen are detected at extremely low exit angles near 0° (the grazing exit condition). This technique requires the analytical objects exist on a flat surface. Therefore, the GE-EPMA analysis has been used only for the analysis of particles or a thin film on a flat substrate so that there were only few applications for practical analysis. As a new application, we have carried out GE-EPMA analysis of ∼0.2-μm inclusions on stainless steel, which appeared to be a projection on the specimen surface with chemical etching. The GE-EPMA quantitative results were in excellent agreement with those of inclusions that were extracted from the stainless steel and analyzed by EPMA with conventional exit condition (30°). This method could be, therefore, applied to the analysis of the submicrometer inclusion in a wide variety of metallic materials if the inclusion appears to be a projection with chemical etching treatment.

Grazing exit electron probe microanalysis (GE-EPMA) is a new method of EPMA[1] in which characteristic X-rays emitted from a specimen are selectively detected with the grazing exit condition (extremely low exit angles near 0°). The GE-EPMA analysis method, then, requires the analytical objects exist on a flat surface. It was reported that GE-EPMA is effective for the analysis of small particles or a thin film on a flat substrate.[1−3] We have, then, applied the GE-EPMA method to the analysis of submicrometer inclusions on an etched stainless steel surface (the major elements of the stainless steel were iron, chromium, and nickel) as a new application.

The existence of inclusions in metallic materials affects the properties of the materials. For example, the ductility of the inclusions in molten Fe−Ni alloy affects the workability of the alloy.[4] The forms of inclusions in free-cutting steel affect the machinability of the steel.[5] Such properties of the inclusions depend on the compositions of the inclusions.[4−5] Therefore, wif we could know the compositions of the inclusions, we could know the properties of the inclusion precisely. Such inclusions have been commonly analyzed by the following methods. They were collected after dissolving the matrix chemically and analyzed by atomic absorption spectrometry or combustion/infrared absorption method[6] or they were collected from the stainless steel by the extraction replica method and analyzed by energy dispersive X-ray spectroscopy (EDS) of a transmission electron microscope (TEM).[7]

We have problems, however, when we analyzed the submicrometer inclusions by the above methods. It is difficult to observe the form and the size of the inclusion when we analyze them by the atomic absorption spectrometry or the combustion/infrared absorption method. Although we can analyze the inclusions without the influence of the matrix by TEM using the extraction replica method, the area analyzed is still limited (∼2 mm^2). On the other hand, EPMA could be used for the inclusion analysis of the comparatively large area (∼20 mm^2) of a sample.[8] However, when an inclusion of <1 μm diameter is analyzed by EPMA, characteristic X-rays from the matrix elements are excited by an electron beam that penetrates through the inclusion and reaches the matrix. We, then, detect not only X-rays emitted from the inclusion but also X-rays emitted from the matrix. The X-rays from the matrix disturb the accurate element identification and the quantitative analysis of the components of the inclusion. Therefore, we have applied the GE-EPMA method to the analysis of submicrometer inclusions because we expected that X-rays emitted from only the inclusion could be detected by the proposed method as stated below.

Inclusions in stainless steel are nonmetallic materials, such as an oxide, a sulfide, etc. When the stainless steel surface is etched chemically and only the matrix is dissolved, the inclusions are projected on the etched surface. Since this relationship between the etched surface and the inclusion on it is similar to that between the flat substrate and the particle sitting on it, we expected that we could analyze such inclusions by the GE-EPMA method. The surface of the etched matrix is, however, not flat, because of a roughness that depends on the microstructure of the stainless steel, although the GE-EPMA analysis method requires that analytical objects exist on a flat surface. In this work, we compare the analytical results of submicrometer inclusions on an etched stainless surface by GE-EPMA analysis with those

(1) Tsuji, K.; Wagatsuma, K.; Nullens, R.; Van Grieken, R. E. *Anal. Chem*. **1999**, *71*, 2497−2501.
(2) Tsuji, K.; Murakami, Y.; Wagastuma, K.; Love, G.. X-ray *Spectrometry* **2001**, *30*, 123−126.
(3) Spolnik, Z.; Zhang, J.; Wagatsuma, K.; Tsuji, K. *Anal. Chim. Acta* **2002**, *455*, 245−252.
(4) Nishi, T.; Shinme, K. *Tetsu to Hagane* **1998**, *84*, 97−102.
(5) Bhattacharya, D. *Met. Trans. A* **1991**, *12A*, 973−985.
(6) Narita, K. *Tetsu to Hagane*, **1987**, *73*, 67−83.
(7) Zhang, Z.; Farrar, R. A. *Mat. Sci. Technol.* **1996**, *12*, 237−260.
(8) Miki, Y.; Kitaoka, H.; Sakuraya, T.; Fujii, T, *ISIJ Int.* **1992**, *32*, 142−149.

10.1021/ac020740l CCC: $25.00
Published on Web 06/20/2003

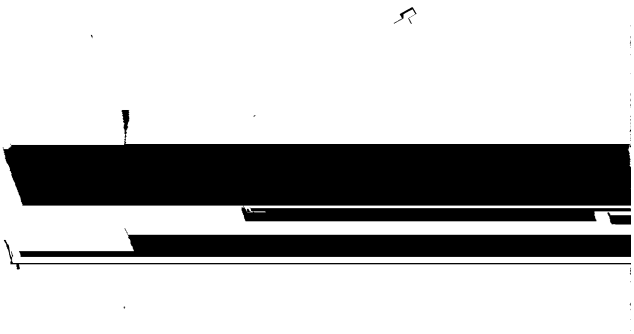

Figure 1. Adjustment of the exit angle by shifting the position of a specimen along the *z* axis.

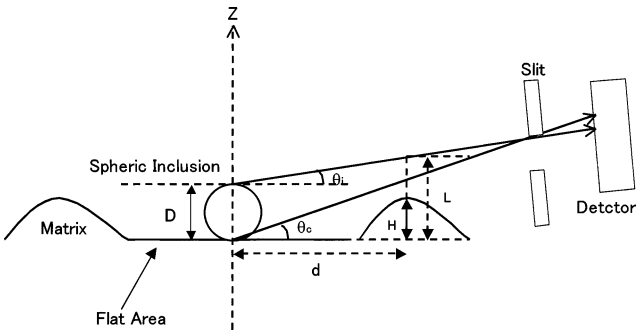

Figure 2. Schematic drawings of the detector, the slit, the inclusion on the flat part of the matrix, and the projection part of the matrix.

of the conventional EPMA method. We then discuss the effectiveness of the element identification and the quantitative analysis of the components of the submicrometer inclusions on the etched stainless steel by GE-EPMA analysis.

EXPERIMENTAL SECTION

Apparatus. The analyses of the samples were carried out by an EDS-SEM: JSM-5400 (JEOL, Tokyo, Japan). The correction procedures of the ZAF correction used in the EDS system are as follows: The atomic number correction *Z* is from the Philibert-Tixier method.[9] The absorption correction *A* is from the Heinrich-Yakowitz method.[10] The fluorescence correction *F* is from the Reed method.[11] The geometry between the detector and the sample are shown in Figure 1. A 3.6-mm-diameter collimator was set in front of the detector. A 0.3-mm-wide leaden slit (the line DG in Figure 1) was fit on the collimator to reduce the angle range of the X-rays detected by the X-ray detector for the GE-EPMA analysis. The distance between the front face of the slit and the detector (the line BE in Figure 1) was 12.8 mm. Point A in Figure 1 is the analysis point with a working distance of 20 mm (the standard working distance of the EDS system.). The distance between the detector and the sample (line AB in Figure 1) was 48 mm. Line AB makes an angle of 30° to the horizontal plane (line AC in Figure 1).

Adjustment of the Exit Angle of Characteristic X-rays. We used a new convenient adjustment method of the exit angles of the characteristic X-rays to obtain the exit angles that satisfy the grazing exit condition when we carried out the analyses using a conventional EDS-SEM.[12] In this method, the exit angles of the X-rays were adjusted by shifting the sample position along the electron beam direction (*z* axis). A shift of the specimen along the *z* axis was called ΔZ in this work. We defined ΔZ as equal to 0 when the working distance was 20 mm. The sample was put on the brass stand inclined 28° from the line AC in Figure 1.[1] We can detect the X-rays of the exit angle near 0° by only a small shift of the specimen using this brass stand.[1] When the specimen was shifted up ($+\Delta Z$), the exit angle $\theta_{\Delta Z}$ was decreased, as shown in Figure 1.

An Analysis of a Cluster ZnO Particles Sitting on a Flat Stainless Steel. We searched for the grazing exit condition of the flat stainless steel as follows. The stainless steel was polished to a mirror surface using alumina particles of 0.05 μm. The ZnO particles of 0.2-μm diameter were scattered on the polished surface in the atmosphere. The major parts of the particles were blown by an air blower so that the surface was dotted with the clusters where several ZnO particles clustered. We measured the intensities of O K$-$L$_3$ and Zn L$_3-$M$_5$ emitted from the cluster ZnO particles and Cr K$-$L$_3$, Fe K$-$L$_3$,and Ni K$-$L$_3$ emitted from the stainless steel as a function of ΔZ when the cluster ZnO particles sitting on the flat stainless steel were analyzed with the point analysis by the EPMA method. From this result, the grazing exit condition ΔZ, where only the X-rays emitted from the cluster ZnO particles were detected, could be found.

Analyses of Submicrometer Inclusions on an Etched Stainless Steel. After the surface of the stainless steel was polished with 0.05-mm alumina particles, the specimen surface was etched by anodic electrolysis in a solution of 3.5 wt % oxalic acid for 30 s at 5 V. The inclusions projected on the etched surface were analyzed using the conventional exit condition (30°) and the grazing exit condition, which was obtained by the measurement of the cluster ZnO particles sitting on the flat stainless steel as stated above, with the point analyses. In the GE-EPMA analysis, nine submicrometer inclusions were analyzed.

After a stainless surface is etched chemically, the roughness that depends on the microstructure of the stainless steel appears on the etched surface. The schematic drawings of the detector, the slit, the inclusion on the flat part of the matrix, and the projection part of the matrix are shown in Figure 2. We discuss the height of the roughness, where the X-rays emitted from the inclusion could reach the detector without being intercepted by the roughness, as follows. The width of the slit in Figure 2 was 0.3 mm; the inclusions that were analyzed had diameters of <1 μm. The distance between the inclusion and the slit was much longer than the diameter of the inclusion. Therefore, we could put θi equal to θc; then

$$H < d \tan \theta \Delta c + D \qquad (1)$$

When the condition of eq 1 is satisfied, GE-EPMA measurements can be performed.

Analyses of Inclusions Extracted from the Stainless Steel Matrix. We expected that the intensities of the characteristic X-ray of the inclusion elements in the GE-EPMA X-ray spectrum are increased by the fluorescence X-rays of the inclusion elements

(9) Philibert, J.; Tixier, R. *Brit. J. Appl. Phys.* **1968**, *1*, 695.
(10) Heinrich, K. F. J.; Yakowitz, H. *Microchim. Acta* **1968**, *5*, 905.
(11) Reed, S. J. B. *Brit. J. Appl. Phys.* **1965**, *16*, 913.
(12) Awane, T.; Kimura, T.; Suzuki, J.; Nishida, K.; Ishikawa, N.; Tanuma, S. *J. Surf. Anal.* **2002**, *9*, 171−177.

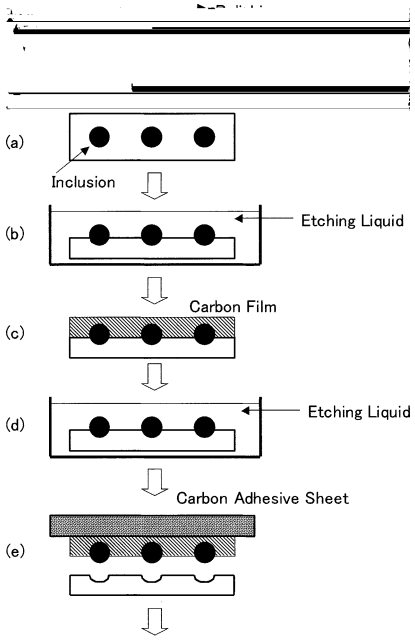

Figure 3. Fabrication process of extraction replica: (a) polishing the specimen, (b) etching the specimen to make the inclusions appear on the surface, (c) covering the etched surface with carbon, (d) etching the specimen so as not to peel the carbon film off the specimen, (e) peeling the carbon film with the adhesive carbon sheet, and (f) setting the adhesive carbon sheet with the carbon film on a sample holder.

excited by the X-rays emitted from the matrix elements in the stainless steel. Inclusions extracted from the stainless steel were, therefore, analyzed with the conventional exit condition (30°) to remove the matrix effect. We then compared the results of the GE-EPMA analyses with those of the above methods. Six submicrometer inclusions were analyzed with point analysis by the EPMA method.

We used an extraction replica method to extract the inclusions from the stainless steel.[12] The fabrication process of the extraction method was shown in Figure 3. In this work, the etchings in Figure 3b,d were performed by anodic electrolysis in a water solution of 3.5 wt % oxalic acid at 5 V. Inclusions on a carbon film were fixed on an adhesive carbon sheet consisting of mainly carbon and oxygen.

Calculation of the Exit Angles. Since the ΔZ is related to the exit angle $\theta_{\Delta Z}$, we can calculate the exit angle from the geometry shown in Figure 1 by the following equation.

$$\theta_{\Delta Z} = \tan^{-1}\frac{18.3 - \Delta Z}{28.9} - 28 \qquad (2)$$

The details of the calculation will be published elsewhere.[13]

The Measurement Condition. The measurement conditions of the analysis of a cluster of ZnO particles sitting on the flat stainless steel surface were the acceleration voltage, 15 kV; probe current, 1 nA; and collection time, 100 s. The measurement conditions of the analysis using the conventional exit condition of the inclusion on the etched stainless steel surface were the acceleration voltage, 15 kV; probe current, 0.35 nA; and collection time, 100 s. The measurement conditions of the analysis with grazing exit condition of the inclusion on the etched stainless steel surface were the acceleration voltage, 15 kV; probe current, 1 nA; and collection time, 600 s. The measurement conditions of the analysis of the inclusion extracted from the stainless steel by the extraction method shown in Figure 3 were the acceleration voltage, 15 kV; probe current, 0.35 nA; and collection time, 200 s.

(13) Awane, T.; Kimura, T. Submitted.

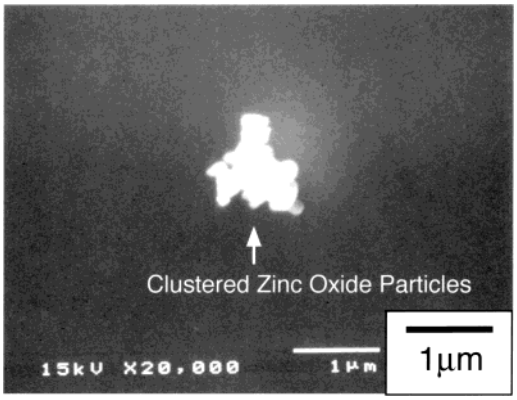

Figure 4. SEM image of a cluster of ZnO particles on the polished stainless steel.

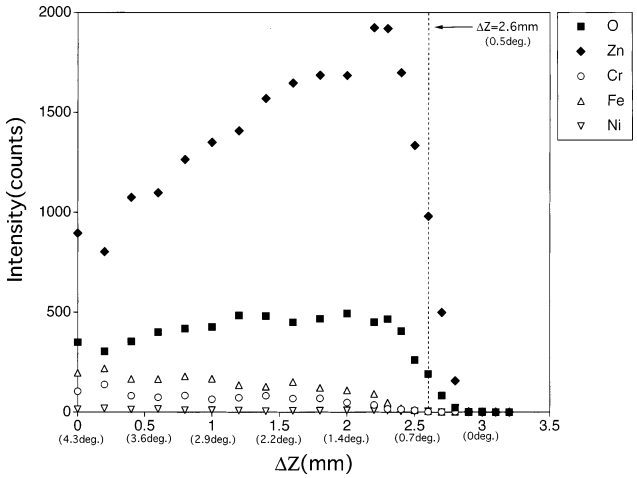

Figure 5. X-ray intensities of O K−L_3, Zn L_3−M_5, Cr K−L_3, Fe K−L_3, and Ni K−L_3 as functions of ΔZ.

RESULTS AND DISCUSSION

GE-EPMA Analysis of a Cluster of ZnO Particles on Flat Stainless Steel. The SEM image of the cluster of ZnO particles on the flat surface of the stainless steel is shown in Figure 4. The diameter of the cluster was ~1 μm. This cluster was isolated from the other particles or clusters. Figure 5 shows the intensities of Zn L_3−M_5 and O K−L_3 emitted from the particle and those of K−L_3 lines of Fe, Cr, and Ni emitted from the stainless steel as a function of ΔZ. When ΔZ was >2.6 mm (detection angle = 0.5°), X-rays emitted from the cluster ZnO particles were detected. In this case, the X-rays from the element in the stainless steel could not be detected. When ΔZ was 3 mm (detection angle = 0°), X-rays emitted from the ZnO particles were not detected. The exit angle of the X-rays therefore satisfied the grazing exit condition when ΔZ was from 2.6 to 3.0 mm (~0.5 to 0°).

The Images of the Submicrometer Inclusions on the Etched Stainless Steel and the Extracted Inclusions. Figure 6a,b shows the typical SEM images of the microstructure and

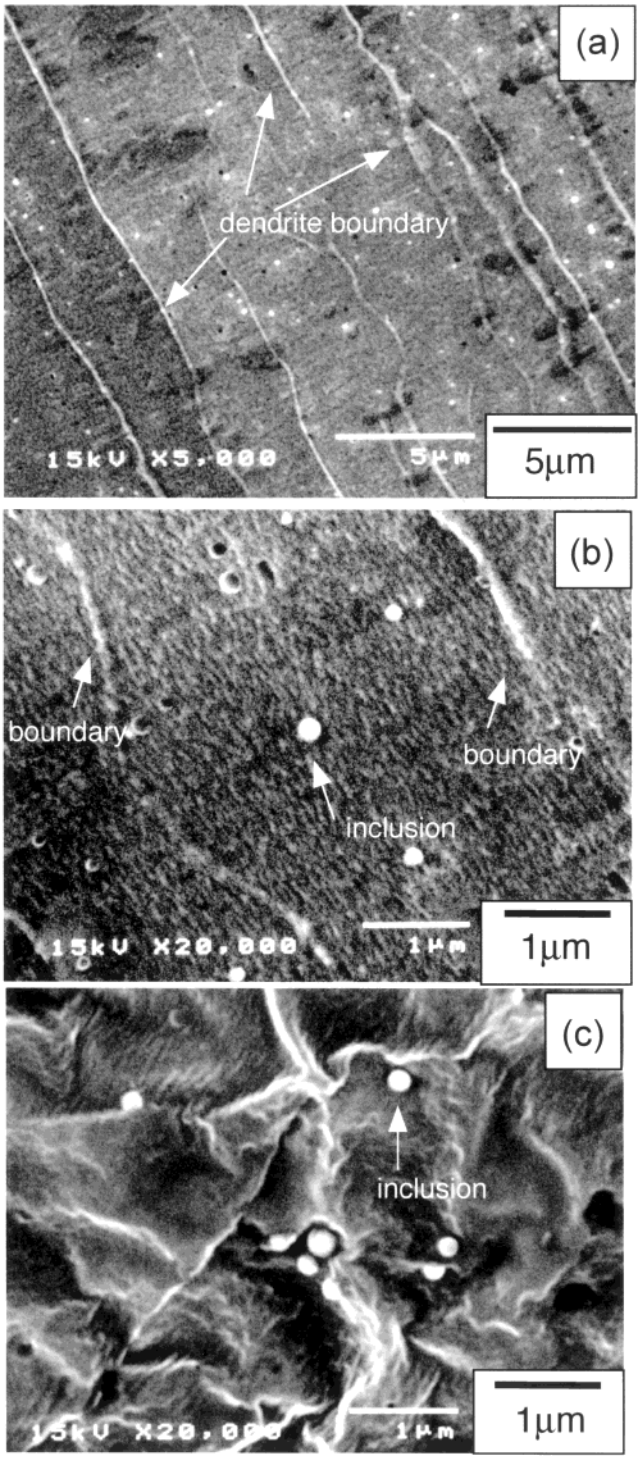

Figure 6. SEM images of the microstructure of the stainless steel and the submicrometer inclusions: (a) the microstructure, (b) the submicrometer inclusions, and (c) the inclusions extracted from the matrix.

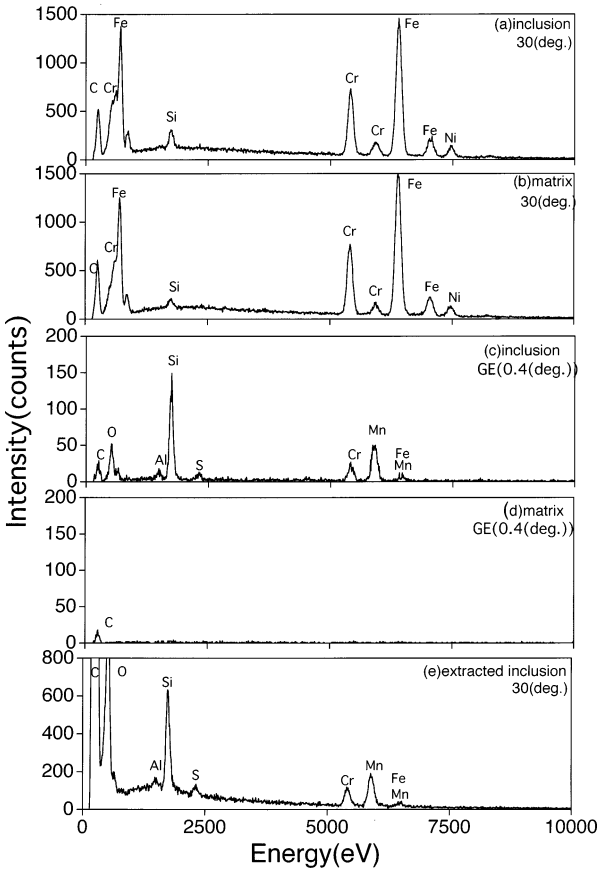

Figure 7. X-ray spectra of the inclusion and the matrix: (a) the inclusion under the conventional exit condition (30°), (b) the matrix under the conventional exit condition, (c) the inclusion under the grazing exit condition (ΔZ = 2.65 mm, $\theta_{\Delta Z}$ = 0.4°), (d) the matrix under the grazing exit condition, (e) the extracted inclusion under the conventional exit condition.

spherical inclusions, the diameters of which were ~0.2 μm. The microstructure was dendritic, and the parts surrounded by the dendrite boundaries were comparatively flat. The inclusions and the dendrite boundaries, which appeared as a result of the chemical etching, were projected onto the flat area of the matrix. The inclusions shown in Figure 6 might be nonmetallic materials, as stated in the Introduction, and there might be segregation of Cr and Ni in the dendrite boundary shown in Figure 6.[14] Therefore, the inclusions and the dendrite boundary might be more difficult to dissolve chemically, as compared to the flat matrix parts. Figure 6c shows a typical SEM image of spherical inclusions (~0.2 μm), which were extracted from the stainless steel with the extraction method shown in Figure 3.

GE-EPMA Analyses of the Inclusions on the Etched Stainless Steel Surface. Figure 7a,b shows X-ray spectra of the elements of the submicrometer inclusion (~0.2 μm) and those of the stainless steel matrix measured with a conventional measured condition (exit angles = 30°). In the spectrum of the inclusion shown in Figure 7a, X-rays appear not only from the elements in inclusion but also from the matrix elements. We could not, therefore, obtain an accurate elemental identification and quantitative analysis from this spectrum. Figure 7c,d shows X-ray spectra of the inclusion (~0.2 μm diameter) and those of the matrix near the inclusion measured using the grazing exit condition (Δz = 2.65 mm, $\theta_{\Delta Z}$ = 0.4°). The peaks of the O K−L_3, Al K−L_3, Si K−L_3, S K−L_3, Cr K−L_3, Mn K−L_3, and Fe K−L_3 could be seen in the X-ray spectrum shown in Figure 7c. The X-rays of carbon in the spectrum of Figure 7c were mainly emitted from carbon contamination induced by the electron beam. On the other hand, the X-rays from the major elements Fe, Cr, and Ni in the matrix were

(14) Inoue, H.; Koseki, T.; Ohkita, S.; Fuji, M., J. *Jpn. Welding Soc.* **1997**, *15*, 77−87.

hardly detected, as shown in Figure 7d. We have, therefore, found that the inclusion, which was analyzed using the grazing exit condition, consisted of O, Al, Si, S, Cr, Mn, and Fe. The X-ray of carbon and oxygen in the spectrum of Figure 7e was mainly emitted from the carbon adhesive sheet used for the extraction method shown in Figure 3.

The P/B ratio of the Si K−L_3 peak in the GE-EPMA spectrum shown in Figure 7c was 22, and it was much higher when compared to those of the conventional EPMA spectrum in Figure 7a (P/B ratio = 2.5) and 7e (P/B ratio = 4.8) as a result of extremely low background under the grazing exit condition. The backgrounds in the conventional EPMA spectra shown in Figure 7a,e were mainly a result of the continuous X-rays emitted from the interior of the samples. On the other hand, since the continuous X-rays emitted from the interior of the sample were hardly detected under the grazing exit condition, the background intensity in Figure 7c was lower, as compared to those in Figure 7a,e.

We carried out the standardless quantitative analyses of the elements of the inclusions using the spectra of the GE-EPMA and those of the inclusions extracted from the stainless steel with the extraction method, as shown in Figure 3. In this analysis, the oxygen contents of the inclusions were determined from the metallic components' concentration from the chemical equivalence method. The standardless ZAF correction procedure used for these quantitative analyses (See Experimental Section, apparatus) was developed for the correction in the bulk analysis. Therefore, we could not obtain the accurate concentrations of the inclusions using this ZAF correction method, even if we carried out the quantitative analyses of the inclusions extracted from the stainless steel. We could, however, compare the quantitative results by the GE-EPMA analysis with those of the extracted inclusions, which were matrix-free analyses. We could, as a result, discuss the difference between the quantitative results and the variation of the quantitative results of the GE-EPMA analysis by the fluorescence X-rays of the inclusion elements excited by the X-rays emitted from the stainless steel matrix elements.

Table 1 shows the analytical results of the inclusions, together with the standard deviations by the GE-EPMA analysis and those of inclusions extracted from the stainless steel using the conventional exit condition. The quantitative results of aluminum (Al_2O3), silicon (SiO_2), sulfur (SO_3), chromium (Cr_2O_3), and manganese (MnO) contents in the inclusions detected by the GE-EPMA analysis are in excellent agreement with those of the extracted inclusions. The difference between the analytical results by the GE-EPMA analysis and those of extracted inclusions were <6.9% for relative errors. Furthermore, these results showed the small statistical deviation, as listed in Table 1. From these agreements, we found that the intensities of the characteristic X-rays of the inclusion elements in the GE-EPMA spectra were not affected by the fluorescence X-rays of the inclusion elements excited by the X-rays emitted from the stainless steel matrix elements. Thus, these results indicate that the proposed GE-EPMA method could be used for practical analyses of inclusions in metallic materials.

There were some inclusions in which iron was detected and other inclusions in which iron was not detected in both the analytical results by the GE-EPMA analysis and those of extracted inclusions with the conventional exit condition. The analytical

Table 1. Results of the Determination of the Concentrations of the Inclusions

	concn (wt %)					
inclusion no.	Al_2O_3	SiO_2	SO_3	Cr_2O_3	MnO	Fe_2O_3
			(A) GE-EPMA			
1	2.2	37.4	4.2	14.1	40.3	2
2	2.2	35.4	2.9	15.2	40.0	4
3	2.0	39.6	3.1	17.0	38.3	nd
4	3.2	41.9	2.2	15.0	37.6	nd
5	3.1	39.2	3.5	14.9	30.1	9
6	2.2	40.5	3.2	13.2	41.0	nd
7	1.6	41.0	3.6	16.7	37.2	nd
8	2.6	37.4	1.3	15.7	43.1	nd
9	2.4	39.0	3.9	16.0	31.9	7
av	2.4	39.0	3.1	15.3	37.7	(2.4)
SD	0.5	2.0	0.9	1.2	4.2	_
			(B) Extracted Inclusions			
1	2.0	45.0	1.5	17.4	34.2	nd
2	4.2	38.6	3.3	14.0	39.9	nd
3	2.4	39.7	5.6	15.6	36.8	nd
4	3.2	40.2	4.3	19.0	33.3	nd
5	1.7	38.0	4.4	17.9	37.1	1
6	nd	48.7	nd	12.5	37.7	1
av	2.3	41.7	3.2	16.1	36.5	(0.3)
SD	1.3	4.2	1.9	2.5	2.4	-

results of iron (Fe_2O_3) were not reliable, because its analysis line (Fe K−L_3) was close to that of Mn K−M_3, which was a major component of the inclusion, and they were also low concentrations.

Detection Limit of the Inclusion Size in the GE-EPMA Analysis. In this section, we will discuss the minimum size of inclusion, which could be analyzed by GE-EPMA analysis. The background intensity is extremely low in the GE-EPMA spectrum; the detection limit becomes better if we use a higher beam current and longer analysis time, as compared to the present analysis condition. If we use a field emission gun SEM (FEG-SEM), the beam current can be increased by 20 times (20 nA), and the collection time can be increased up to 3000 s, as compared to the present condition. Then, the intensity could be increased by 100 times, as compared to the present condition.

We define that the 50% intensity of the Si K− L_3 intensity emitted from the silicon contents in the 0.2-μm-diameter inclusion, which was analyzed using the present GE-EPMA analysis condition, was the Si K− L_3 intensity of the detection limit of the GE-EPMA analysis. Since the X-ray intensity is proportional to the volume of the inclusion, we could therefore detect X-rays emitted from a 1/200 volume of an inclusion of 0.2-μm diameter. Then the inclusion size at the detection limit could be estimated as 0.03-μm diameter in the GE-EPMA analysis.

CONCLUSION

We have used a new convenient adjustment method for the exit angles of the characteristic X-rays to obtain the exit angles that satisfy the grazing exit condition when we carried out the analyses using a conventional EDS-SEM.[12] In this method, the exit angles of the X-rays were adjusted by shifting the sample position along the electron beam direction (z axis), as shown in Figure 1. We searched for the grazing exit condition of the flat stainless steel. We, therefore, scattered cluster ZnO particles on the flat stainless steel and analyzed a particle using point analysis.

We then measured the changes of the X-ray intensities of O K−L_3 and Zn L_3−M_5 emitted from the particles and Cr K−L_3, Fe K−L_3, and Ni K−L_3 emitted from the stainless steel as a function of ΔZ, as shown in Figure 5. From Figure 5, we found that the exit angle of the X-rays satisfied the grazing exit condition when ΔZ was from 2.6 to 3.0 mm (∼0.5 to 0°). We have carried out the GE-EPMA analysis of the submicrometer inclusions (∼0.2 μm), which appeared to be projections on the specimen surface after chemical etching. We then detected the X-rays of O, Al, Si, S, Cr, Mn, and Fe emitted from only the inclusion. The quantitative results of aluminum (Al_2O3), silicon (SiO_2), sulfur (SO_3), chromium (Cr_2O_3), and manganese (MnO) contents in the inclusions detected by the GE-EPMA analysis are in excellent agreement with those of the extracted inclusions. The differences between the analytical results by the GE-EPMA analysis and those of extracted inclusions were less than 6.9% for relative errors. Furthermore, these results showed a small statistical deviation, as listed in Table 1. The inclusion size of the detection limit could be estimated as 0.03-μm diameter in the GE-EPMA analysis if we used a higher beam current and longer collection time using FE-SEM. These results indicate that the proposed GE-EPMA method could be used for practical analyses of inclusions in metallic materials.

ACKNOWLEDGMENT

T.A. thanks Professor K. Tsuji (Osaka City University) for providing references, Dr. M. Kasugai (NIMS) for providing the specimen, and Dr. M. Nakanishi (JEOL. Engineering. Ltd) for the useful comments for the EDS detector. We also thank Dr. V. Nehasil and Mr. T. Hrncir (Charles University, Czech Republic) for their proofreading of this paper.

Received for review December 2, 2002. Accepted April 24, 2003.

AC020740L